


Biointerfacial Analysis of HEK293 Cells in Contact with Hydrogels based on Poly-*N*-Isopropylacrylamide and Copolymers

Virginia Capella, Ana C. Liaudat, Martin F. Broglia, Cesar A. Barbero, Pablo Bosch, Nancy Rodríguez, and Claudia R. Rivarola*

Several researches have demonstrated that synthetic hydrogels can mimic the mechanical and physicochemical properties of native extracellular matrices and act as cell-scaffold. The biointerface can influence over tissue activities such as adhesion, signaling, cell–cell communications, and proliferation. In this work, the behavior of human embryonic kidney cells (HEK293) in contact with hydrogel surfaces based on poly-*N*-isopropylacrylamide (PNIPAM) and copolymers is studied. Ionic and neutral hydrogel surfaces are synthesized by free radical polymerization and characterized by Fourier-transform infrared spectroscopy, swelling capacity, and wettability at culture conditions. Viability, proliferation, and bioadhesive capacity are analyzed by 3-(4,5-dimethylthiazol-2-yl)-2,5-diphenyltetrazolium bromide and Neutral Red assays, [³H]-thymidine technique, Acridine Orange and Hoechst dye. Noncytotoxic and proliferative effects are observed in all cases. HEK293 cells are mainly adapted and adhered on neutral and low ionic charge surfaces showing typical cell morphology, and normal mitotic rates. While, lower adhesion, abnormal nuclear and cytoplasmic morphologies with mitotic/fragmentation processes are observed after contact with high ionic surfaces. The cellular cycle after culture on PNIPAM, assessed by flow cytometry, is not affected regarding control surfaces (polystyrene). Therefore, hydrogel surfaces with neutral and low ionic charges can be apt to in vitro tissue development and possible applications of biomedical treatments.

V. Capella, A. C. Liaudat, P. Bosch, N. Rodríguez
Molecular Biology Department
Faculty of Exact
Physical Chemical and Natural Sciences
Institute of Environmental Biotechnology and Health (INBIAS)
National University of Rio Cuarto (UNRC)-National Council of Scientific
and Technical Research (CONICET)
National Route 36 KM 601, X5804ZAB Rio Cuarto, Córdoba, Argentina
V. Capella, M. F. Broglia, C. A. Barbero, C. R. Rivarola
Chemistry Department
Faculty of Exact
Physical-Chemical and Natural Sciences
Institute of Research in Energy Technologies
and Advanced Materials (IITEMA)
National University of Rio Cuarto (UNRC)-National Council of Scientific
and Technical Research (CONICET)
National Route 36 KM 601, X5804ZAB Rio Cuarto, Córdoba, Argentina
E-mail: crivarola@exa.unrc.edu.ar

 The ORCID identification number(s) for the author(s) of this article can be found under <https://doi.org/10.1002/admi.202201162>.

DOI: 10.1002/admi.202201162

1. Introduction

Hydrogels are hydrophilic crosslinked polymers that have the ability to absorb and retain a large amount of water, maintaining macroscopic integrity with wettability, soft and flexible properties, resembling a native extracellular matrix better than other synthetic biomaterials from the mechanical and physiological point of view.^[1–4] For that reason, most of them have a great potential as biomaterials to be applied in the tissue engineering field as well as being used as cell-laden scaffold or in vitro tissue constructs.^[5] It has been demonstrated that the interfacial adhesion between hydrogels and a cells depends on chemical composition of the scaffold material, being able to alter the cellular mechanotransduction process and consequently the tissue development.^[6–8] Several strategies applied on scaffold material to enhance the cell bioadhesion can be performed, such as: the covalent incorporation of biomimetic molecules and/or grown factors to hydrogels,^[9] or through the chemical modification of

surfaces in order to vary the physicochemical properties as hydrophilicity/hydrophobicity.^[10–13]

One of the biocompatible synthetic homopolymers widely studied in the biomedical field is the poly-*N*-isopropylacrylamide (PNIPAM),^[14] which has a coil-globule phase transition at a critical temperature (lower critical solution temperature) of ≈32 °C in water, which is close to human body temperature.^[15] PNIPAM hydrogel and copolymers have shown good biocompatibility in contact with several cell lines such as bovine fetal fibroblast (FFBs),^[12,13] human epithelial colorectal adenocarcinoma cells (Caco-2), and lung cancer cells (Calu-3),^[16] mesenchymal stem cells derived from rat bone marrow (BMMSCs), and human adipose tissue (AT-MSCs).^[17] In recent studies, the absence of PNIPAM cytotoxic effects and the good bioadhesive properties for different cell lines such as FFBs,^[18] murine pre-adipose cells (3T3-L1), human embryonic kidney cells (HEK293), and human carcinoma-derived cells (A549) in contact with this were demonstrated.^[19] On the other hand, studies of one cell line (FFBs) in contact with surfaces of different

chemical composition hydrogels demonstrated that the bioadhesive property also depends on the biointerfacial properties.

It is known that tissues and organs possess different levels of functional and structural complexity and a specific microenvironment, which mainly influence the design of biomaterials from a biological point of view.^[20] This concept has been confirmed by several studies observing that the development of cell systems is highly dependent on the biointerface or physicochemical interactions between the tissue and the scaffold material. Therefore, the design of a biomaterial as a cell scaffold with high biocompatibility and good adhesion requires an analysis of the physicochemical and mechanical attributes of material and the cells behavior in contact with it.^[21]

The kidneys are among the most complex organs in terms of their anatomy–physiology, and the functional relationship of the cells that constitute them with the scaffold has not been fully understood. Interactions between several kidney cells, including epithelial cells, are important for renal tubule formation, and knowing the behavior of each cell type in this process could help to understand the regenerative capacity of the organ.^[22,23] For that reason, the study of behavior of renal origin cells in contact with scaffold surfaces based on hydrogels could give relevant information about new biocompatible materials for future in vitro renal tissue growth. Therefore, a cell line with epithelial morphology and renal origin (HEK293) was selected to analyze the cell–cell and the cell–scaffold biointerfacial interactions.^[24]

Scaffold surfaces based on PNIPAM and hydrogels copolymerized with ionic and no-ionic comonomers (*N*-acryloyl *tris*-(hydroxymethyl)aminomethane (HMA), (3-acrylamidopropyl)trimethylammonium chloride (APTA) and 2-acrylamido-2-methylpropanesulfonic acid (AMPS)) were synthesized and physicochemically characterized. The biological behavior of HEK293 cell line in contact with hydrogels was studied through viability and proliferation assay, as well as cytoplasmic and nuclei morphology. The bioadhesion and its effect on cellular cycle and mitotic/fragmentary index processes were also assessed. Our results provide relevant information regarding the biointerface cells-hydrogels. From interdisciplinary studies about the behavior of cell–matrices systems, it could be possible to select biocompatible scaffold materials apt to apply in future studies that allow us to design renal constructs for therapeutic use.

2. Results and Discussion

2.1. Physicochemical Characterization of Hydrogel Surfaces

The characteristic functional groups of each synthesized hydrogel were verified by Fourier-transform infrared (FTIR) spectroscopy. After synthesis and washing processes, it was possible to observe the absence of functional groups proved by vinylic monomers, such as: an intense absorption band of vinylic hydrogen ($=C-H$) stretching at 2980 cm^{-1} , other intense band corresponding to $C=C$ stretching at 1625 cm^{-1} and the double bands at 990 and 910 cm^{-1} of vinylic hydrogen stretching. The FTIR spectral changes of NIPAM monomer and PNIPAM polymer are shown in the Supporting Information.^[25]

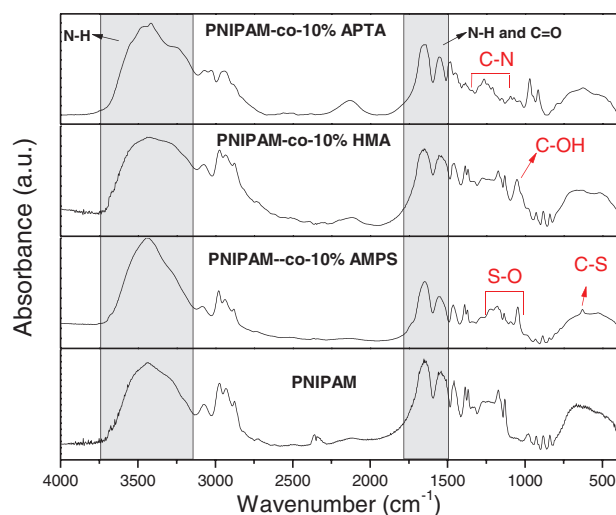


Figure 1. FTIR spectrum of hydrogel matrices: PNIPAM-co-10%APTA, PNIPAM-co-10%HMA, PNIPAM-co-10%AMPS, and PNIPAM. Gray areas indicate commune bands of materials.

The absence of IR absorption bands of vinylic groups indicates that the analyzed material corresponds to the true structure of the synthesized hydrogel. In **Figure 1**, the broadband with maximum centered on 3130 cm^{-1} corresponding to $N-H$ stretching vibration, two strong bands at 1630 cm^{-1} of $C=O$ stretching and 1535 cm^{-1} of $N-H$ bending corresponding to amide groups of hydrogels were observed in all cases.^[26]

The copolymer that contains HMA with hydroxyl groups showed characteristic bands of $O-H$ stretching overlapped with $N-H$ stretching bands widening the band at a range of $3200\text{--}3600\text{ cm}^{-1}$. In addition, a new band at 1040 cm^{-1} corresponding to $C-OH$ stretching of primary alcohols was observed.^[25]

For the copolymer containing AMPS monomeric units, the characteristic bands of the sulfonic groups at $1192\text{--}1040\text{ cm}^{-1}$ (asymmetric and symmetric stretching) and 620 cm^{-1} (st. $C-S$) were observed.^[27]

The quaternary ammonium salt groups (from APTA monomer units) can be differentiated from PNIPAM by the broad and medium intense band of $C-N$ bending at a range of $1300\text{--}1000\text{ cm}^{-1}$.

Maximum swelling percentages ($\%Sw_{(eq)}$) and contact angles of hydrogels were analyzed at different environmental conditions in order to study the temperature and culture medium effects on those properties. Previous works have demonstrated that all synthesized hydrogels, except PNIPAM, have a phase transition temperature overcome $37\text{ }^{\circ}\text{C}$.^[12,13] Therefore, only PNIPAM could be collapsed at culture conditions. It should be noted that the synthetic method of polymerization results in hydrogels with molecular (or nanometric) porosity.^[1]

In **Table 1**, it can be seen that the $\%Sw_{(eq)}$ changed considerably with temperature. At $22\text{ }^{\circ}\text{C}$, the $\%Sw_{(eq)}$ increased for hydrogels with ionic charge (PNIPAM-co-AMPS and PNIPAM-co-APTA) and decreased for hydrogels where the intramolecular hydrogen bonding is more probable (PNIPAM and PNIPAM-co-HMA). A similar tendency was observed at $37\text{ }^{\circ}\text{C}$ but the composition of Dulbecco's modified Eagle's medium (DMEM)

Table 1. Maximum swelling capacity at 22 and 37 °C and contact angles of hydrogel surfaces at 37 °C, all swollen in supplemented DMEM after sterilization process.

Hydrogel	%Sw(eq) in DMEM		Contact angles ^{a)} at 37 °C	
	22 °C	37 °C	H ₂ O	DMEM
PNIPAM	1923.0	89.6	56.9 ± 1.8	69.3 ± 1.0
PNIPAM-co-20%HMA	1541.6	1010.4	55.3 ± 1.7	82.2 ± 0.7
PNIPAM-co-2%AMPS	2886.7	182.3	48.5 ± 0.9	50.0 ± 1.9
PNIPAM-co-10%AMPS	3685.3	2854.3	36.0 ± 0.1	32.0 ± 0.8
PNIPAM-co-3%APTA	2392.3	726.7	56.8 ± 1.9	57.5 ± 2.5
PNIPAM-co-10%APTA	3021.0	213.0	46.9 ± 8.3	35.7 ± 0.1

^{a)} Average values of three measurements per hydrogel.

makes the %Sw(eq) littler than at 22 °C due to difference osmotic. In addition to the medium effect, the higher change of %Sw(eq) was observed to PNIPAM because this collapses over 32 °C.^[12]

After the sterilization process, the wettability characteristics of hydrogel surfaces were analyzed in aqueous and DMEM-10%FBS medium (DMEM supplemented with 10% of fetal bovine serum) at 37 °C, through the measurement of static contact angle formed between a water drop and a surface. It is known that if the contact angle value is less than 90°, the surface is hydrophilic whereas if it is greater than 90°, it is hydrophobic. Surfaces with contact angle between 150° and 180° are called superhydrophobics.^[28]

According to the results in Table 1, the contact angles of surface change from water to supplemented DMEM medium at 37 °C provoking a slight increase of surface hydrophobicity, except for hydrogel surfaces with 10% ionic charges where the contact angle decreased. The highest observed contact angle for PNIPAM-co-20%HMA could be due to the intramolecular interactions of the hydroxyl groups, which could be not exposed to the surface and therefore will make it more hydrophobic. While for PNIPAM-co-10%AMPS and PNIPAM-co-10%APTA, it is possible that the ionic charges are exposed outside surface contributing to formation of a hydration layer, thus becoming in more hydrophilic surfaces.

Therefore, the results indicate that the culture conditions (37 °C and DMEM) considerably affect the %Sw_(eq) (decreasing) and superficial wettability, highlighting the effects for higher ionic charge surfaces.

2.2. Cytotoxicity and Cell Proliferation Studies

Biocompatibility of materials is first evaluated by cytotoxicity assays. HEK293 cells were exposed over each synthesized hydrogel and the cytotoxicity was studied by 3-(4,5-dimethylthiazol-2-yl)-2,5-diphenyltetrazolium bromide (MTT) and Neutral Red uptake assays, after a period of 48 and 96 h (Figure 2). Both staining assays were carried out to assess safety through mitochondrial enzyme activity and integrity of cell lysosomes, respectively. Negative and positive (dimethyl sulfoxide (DMSO):DMEM-10%FBS (1:9), highly cytotoxic) controls were included to validate the viability protocols.

At both culture times, neither alteration in mitochondrial activity (Figure 2A,B) nor in lysosomal level (Figure 2C,D) was observed for all hydrogels, compared to the negative control. Furthermore, the obtained absorbance values were significantly higher than those obtained with DMSO:DMEM-10%FBS (1:9), confirming the absence of cytotoxicity for PNIPAM and copolymers.

On the other hand, the [³H]-thymidine assay gives information about cell proliferation, taking into account the incorporation of this labeled nucleotide in the DNA synthesized in each mitotic cell division. Therefore, this allows analyzing whether the cell cycle is progressing correctly or if there is any alteration in it due to the presence of an external factor, such as the contact with hydrogels. In Figure 3, the proliferation of HEK293 cells exposure at 24 and 48 h of hydrogels can be seen. The counts per minute (cpm) rates indicate that the amount of incorporated nucleotide decreases in the presence of hydrogels after 24 h compared to control cells, being only statistically significant for PNIPAM-co-10%AMPS and PNIPAM-co-20%HMA. However, the proliferation rates are normalized at 48 h with respect to the control. Although, PNIPAM indicates a slight decrease compared to the rest of hydrogels, it did not show any significant difference.

The results indicate that these cells have the capability to proliferate in the presence of these hydrogels without cell cycle affection. This confirms similar biologic behaviors observed about different cell-loaded material systems. Previous studies demonstrated that PNIPAM films do not have cytotoxic effects and allow normal proliferative activity on 3T3-L1, HEK293, and A549 cell lines after 96 and 48 h.^[19] It was also demonstrated that PNIPAM, PNIPAM-co-10%AMPS, PNIPAM-co-10%APTA, and PNIPAM-co-20%HMA hydrogels do not cause damage at the level of mitochondrial activity in FFBs after 24 h.^[13] In addition, 3D macroporous PNIPAM have shown a long-time biocompatibility (75 days), allowing cell migration and proliferation inside the matrix.^[18] On the other hand, studies reported by Vihola et al. do not demonstrate evidence of cytotoxicity by MTT and lactate dehydrogenase (LDH) tests when intestinal Caco-2 cells and bronchial Calu-3 cells were cultured in contact with PNIPAM.^[16] As well as, dermal fibroblast MSU-1.1, cervical cancer cells HeLa, human umbilical vein endothelial cells,^[29] and myoblasts C2C12 adhered to PNIPAM thin films did not show cytotoxic effects for 72 h.^[30]

2.3. Cellular Attachment: Biointerfacial Analysis

The bioadhesive property of materials can be estimated by analyzing the cytoplasmic morphology of cells interacting with the scaffold surface. HEK293 behavior and the level of cell attached over hydrogels scaffold and polystyrene surfaces (control) were followed by staining with Acridine Orange after 2 and 5 culture days with partial replacement of medium every 48 h in order to improve cell growth by nutrient provision. The morphology adopted by stained cells was observed by fluorescence microscope.

At 2 culture days (Figure 4A), an epithelial-like phenotype and like-cluster growth (stronger cell-cell cohesion) were observed when HEK293 cells are in contact with a typical

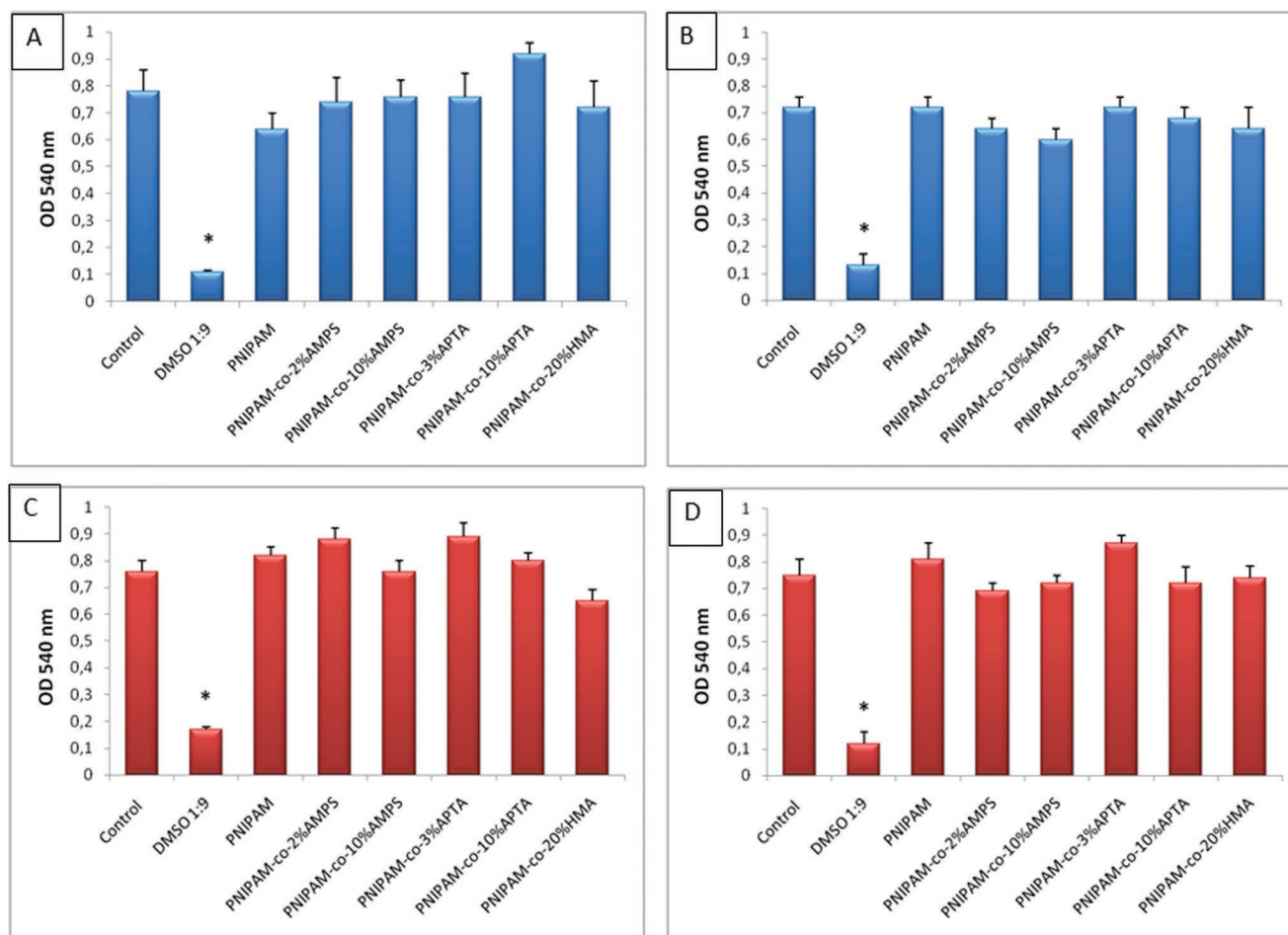


Figure 2. Optical density (OD) of HEK293 cells after A,C) 48 and B,D) 96 h exposed to hydrogels, according to MTT (blue bars) and Neutral Red uptake (red bars) assays. Each bar represents the mean \pm S.E. of three independent replicates. *Statistically significant differences between cytotoxicity positive control (DMSO 1:9) regarding all treatments. Data were analyzed by one way ANOVA and the differences were considered statistically significant with $p < 0.05$.

polystyrene plate.^[31] Similar behavior was observed when these were seeded on PNIPAM surface (Figure 4B), PNIPAM-co-20%HMA (Figure 4C), PNIPAM-co-2%AMPS (Figure 4D), and PNIPAM-co-10%AMPS (Figure 4E) finding cells with epithelial morphology and long cytoplasmic extensions. Typical morphology, resembling fibroblasts, were observed in 2D systems generally due to the effect of forced apical-basal polarity.^[32] In addition, like-cluster cells were formed in a smaller number with tendency to disaggregation and adhesion on the surface. In the case of PNIPAM-co-3%APTA (Figure 4F) and PNIPAM-co-10%APTA (Figure 4G), a tendency to agglomerate with spheroid form was observed, showing an intense cell-cell interaction with respect to control surfaces.

The bioadhesion of HEK293 on hydrogels is clearly highly sensitive to biointerfacial properties and depends on the chemical composition of hydrogels. Comparing the contact angles (inserted on the corresponding cell adhesion image) of control polystyrene surfaces (59.7 ± 0.2) with regard to hydrogel surfaces and the adopted cell morphology in each case, it could be said that the cellular adhesion process depends not only on hydrophobicity but also on ionic charge of surfaces. Compa-

table behavior of cell adhesion was observed over surfaces with hydrophobicity similar to control, except for surfaces with positive charges.

After 5 days in culture, higher cell confluence on the control surface was observed (Figure 5A) with typical epithelial and flattened morphology. For PNIPAM-co-20%HMA (Figure 5C), the cells tended to adopt flattened form although rounded cells were still found. On the other surfaces (Figure 5B,D,F), the cells tended to disperse but cells with rounded morphologies were still observed. However, it is also possible that the high cell confluence does not allow the adhesion to be adequate over surfaces and the cell-cell interactions increase. Only for surfaces of PNIPAM-co-10%APTA and PNIPAM-co-10%AMPS (Figure 5E,G), the cells seem unable to easily adapt to the surface after 5 culture days.

It is known that neutral hydrogels favor the cell attachment and the development of monolayers with typical cytoplasmic morphologies of several cell types.^[16,17,19,29,33] This could also possibly be attributed to the absorption of constituents of culture medium, as growth factors or proteins, which stimulate attachment and proliferation.^[34] In this case according to the

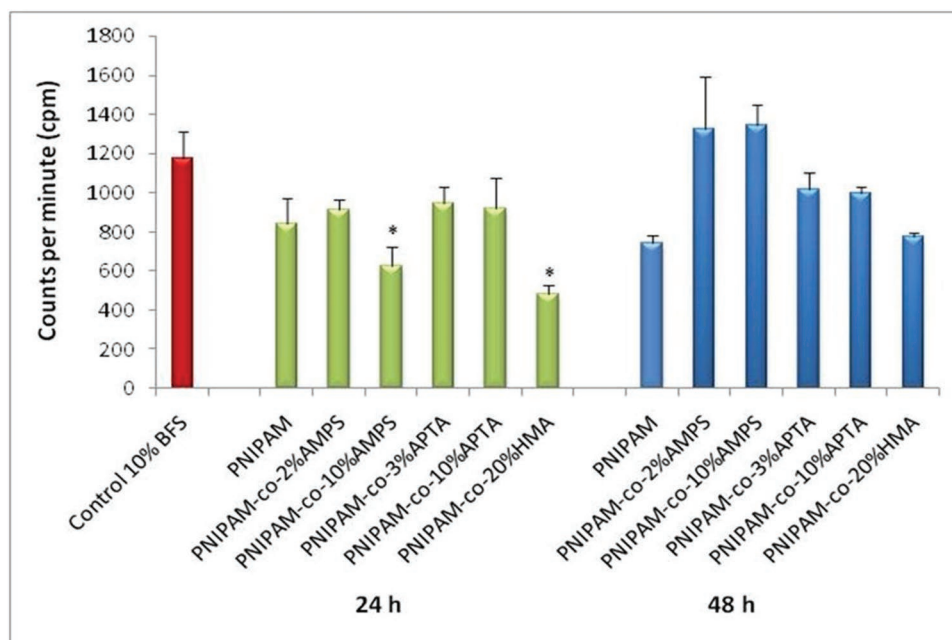


Figure 3. Proliferation of HEK293 cells at 24 and 48 h of exposition to hydrogels, according to [^3H]-thymidine assay. Each bar represents the mean \pm S.E. of three independent replicates, expressed in counts per minute (cpm). Data were analyzed by one way ANOVA and the differences were considered statistically significant with $p < 0.05$. *Statistically significant differences between treatment with hydrogel regarding control 10%FBS.

results of Table 1, the effect of culture medium (salts, proteins, acid amine) regarding wettability was not significant for neutral and low charge surfaces while a level decrease of angle was observed for surfaces with 10% of ionic charges. Therefore, HEK293 mainly adhere and proliferate in contact with hydrogels according to cell-hydrogel biointerfacial characteristics. The changes of cell morphology of HEK293 observed over each surface indicate that the cell tends to adhere over hydrophobic surfaces and to reject surfaces with high ionic content, especially with positive charges. The cell different behaviors are graphically exemplified in **Scheme 1**, varying according to interfacial characteristics of scaffolds.

It is noteworthy that the cell attachment and proliferation depend not only on the superficial characteristics of scaffold but also on the cell line kind. It was observed that FFBs adopted a contracted morphology and were associated in spheroids during 5 days of culture on PNIPAM-co-20%HMA showing poor adherence. While, FFB was adhered on PNIPAM-co-10%APTA shown a typical flattened and spindle-shaped morphology immediately after seeding.^[13] However, in the case of HEK293, a different bioadhesion process for same hydrogels surfaces was observed.

On the other hand, hydrogels with cationic groups in their structure favor the adhesion process and distribution with enhanced cytoskeletal rearrangement in a variety of cells.^[35–37] Results reported by Tan et al. demonstrated that increasing the positive charges of poly-ethylene glycol-diacrylate (PEGDA) hydrogels, the adhesion of preosteoblastic cultures MC3T3-E1 and the expression of genes related with adhesion process increased.^[38] A greater attachment of mesenchymal cells on alginate-poly-amidoamine hydrogels charged positively was also evidenced.^[39] In addition, it is well known that the cells mainly present negative superficial charge due to the presence of gly-

cocalyx in cell membrane,^[40] improving the cell attachment on positive surfaces, especially in those with low positive charge.

In this study, HEK293 cells showed a high tendency to reject highly positive surfaces as PNIPAM-co-10%APTA (Figure 5G) and highly negative as PNIPAM-co-10%AMPS (Figure 5E) where the cells remain agglomerate during the 5 culture days. Although, both ionic surfaces have similar hydrophilicity (Table 1), it seems that the difference in superficial charges considerably affects the adhesion of cell, since in some cases the cells tend to be rejected when there are too many negative charges on surface.^[41] Moreover, higher interfacial hydrophilicity could be recognized by cells as essentially aqueous interfaces, which leads to poor cell attachment.^[42] In several cases, these tend to form cell spheroids, as it was observed in mesenchymal stem cells growing in chitosan and chitosan grafted hyaluronic acid^[43] and with normal human dermal fibroblast on alginate films as well.^[44]

Several researches have demonstrated that cell adhesion or tissue development on biomaterials is dependent on the hydrophobicity/hydrophilicity of the surfaces, indicating that cells have greater proliferation rates on neutral or positively charged surfaces.^[45,46] However, the behavior of HEK293 cells on hydrogel surfaces demonstrates high dependence of amount and positive ionic charges of scaffold surface.

2.4. Nuclear Morphology and Nuclei in Mitosis Analysis

Several cell signals indicate changes in the external environment and are expressed in the cell nucleus. Cell processes such as DNA replication, cell cycle progression, death or alterations in nuclei morphology, among others, are regulated to adapt that change.^[47] Nuclei alterations can be seen through fluorescent Hoechst dye.

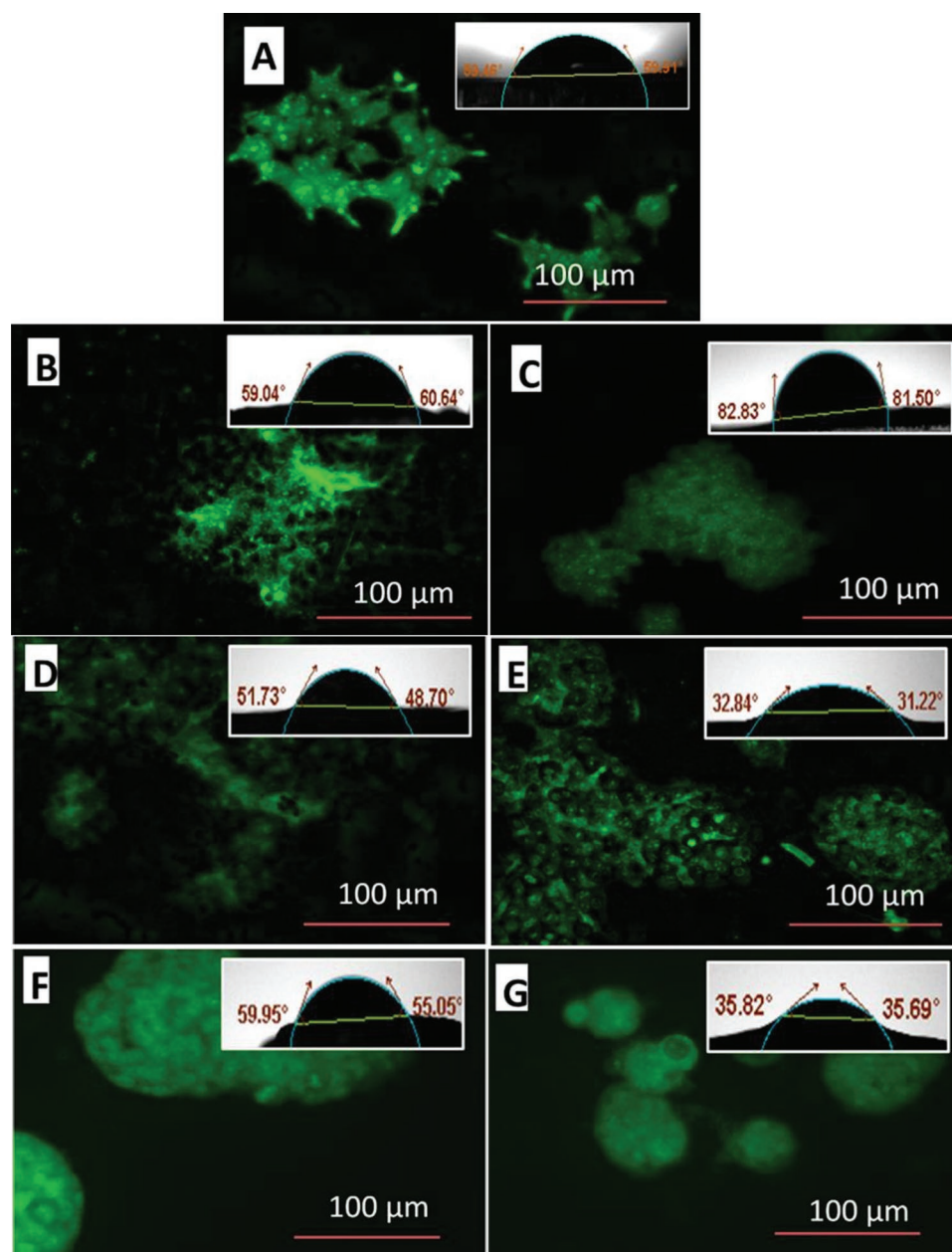


Figure 4. Microphotographs of HEK293 cells stained with Acridine Orange (evidencing cytoplasmic morphology) at day 2 of culture. Inserted: contact angles, respectively. A) Polystyrene surface (control), B) PNIPAM, C) PNIPAM-co-20%HMA, D) PNIPAM-co-2%AMPS, E) PNIPAM-co-10%AMPS, F) PNIPAM-co-3%APTA, G) PNIPAM-co-10%APTA.

Figure 6 shows images of the nuclear morphology of HEK293 cells growing over hydrogel surfaces and the control surface at 2 culture days. Cells adhered to the different surfaces showed a normal (rounded) nuclear morphology, except for those hydrogels copolymerized with 10% of ionic comonomers, AMPS or APTA, where alterations in a large number of nuclei were found (Figure 6E,G). The cell morphologies changed from a typical rounded shape to rectangular or elongated shapes or to highly deformed nuclei presenting extensions with fibroblast-like morphology.

These nuclear shape changes observed in higher wettability hydrogels could be signs of stress due to the recognition of the

hydrogel as foreign material (Figure S2, Supporting Information). At 5 post-seeding days, the number of nuclei present increased with respect to the samples obtained at the second day and a uniform distribution through the whole surface was found, resembling polystyrene control (Figure S3, Supporting Information).

In order to analyze if the properties of surfaces affect the number of living cells during the proliferation process, the fraction of nucleus in mitosis with respect to the total of nuclei present in a sample, and the fraction of fragmented nuclei characteristic event of cell death were calculated.

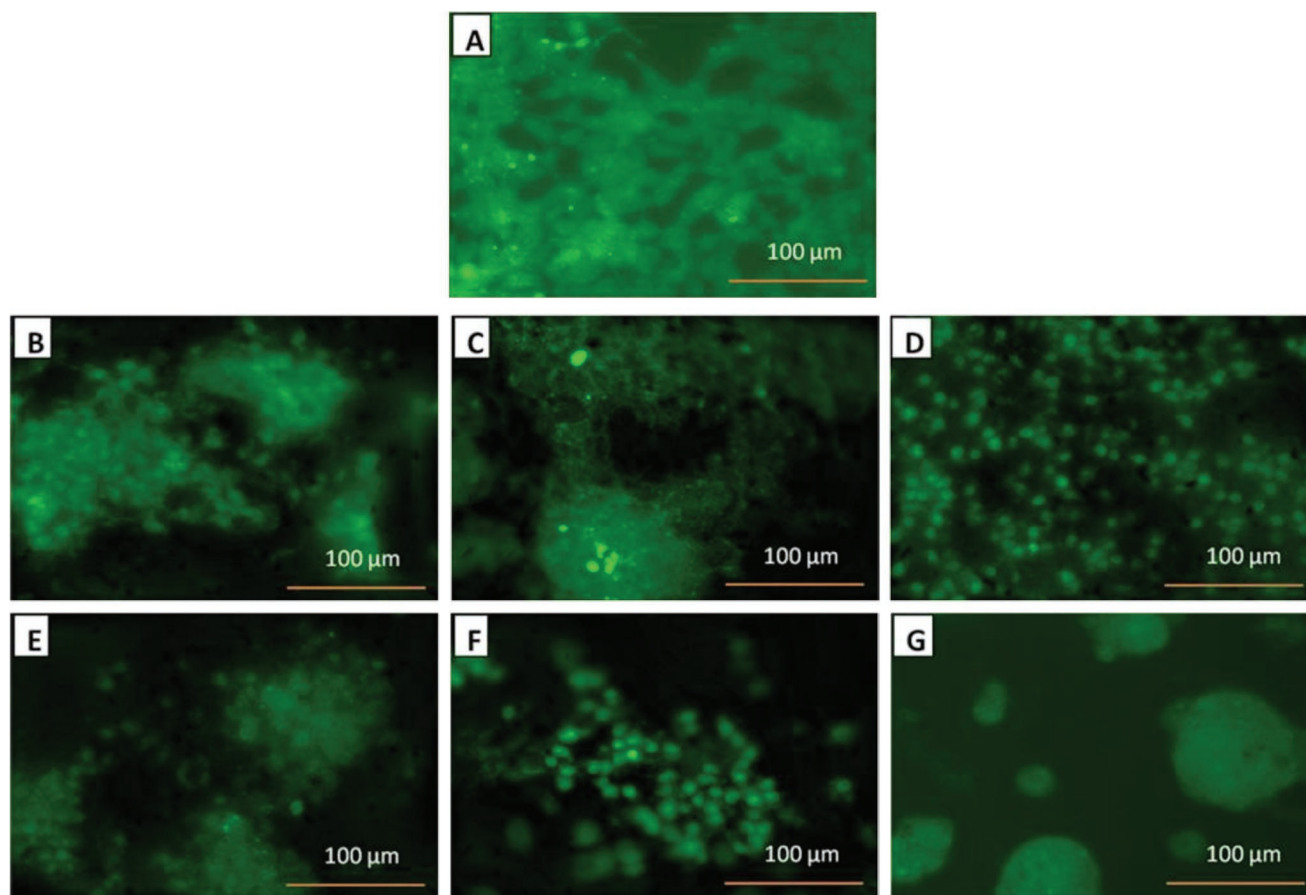
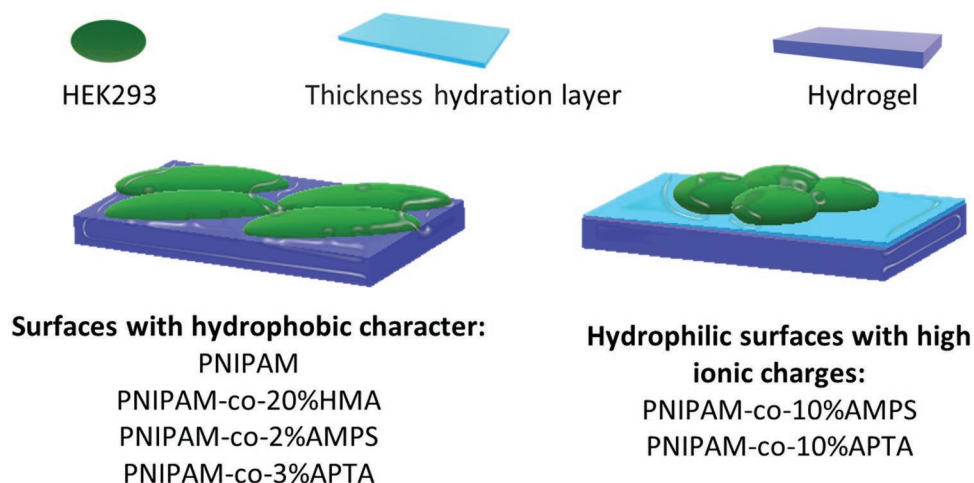


Figure 5. Microphotographs of HEK293 cells stained with Acridine Orange at day 5 of culture. A) Polystyrene surface (control), B) PNIPAM, C) PNIPAM-co-20%HMA, D) PNIPAM-co-2%AMPS, E) PNIPAM-co-10%AMPS, F) PNIPAM-co-3%APTA, G) PNIPAM-co-10%APTA.

Cell growth on polystyrene as control surface indicates a higher number of mitotic cells and lower fragmentation at 2 culture days (Figure 7A). The ratio of fragmented nuclei was significantly higher in hydrogels with anionic and cationic net charge (showing the least fragmentation in PNIPAM-co-10%AMPS) which can be explained by the fact that the cells are still in the

adaptation process on the surface. On 5 culture days (Figure 7B), the fraction of nuclei in mitosis increased, except for PNIPAM-co-10%APTA, being the difference statistically significant. Nevertheless, PNIPAM-co-10%AMPS and PNIPAM-co-10%APTA presented a high and significant fraction of fragmented cells compared to the rest of hydrogels. Furthermore, it was observed



Scheme 1. Graphic representation of HEK293 behaviors (adhesion and morphology) in contact with hydrogel surfaces of different chemical compositions.

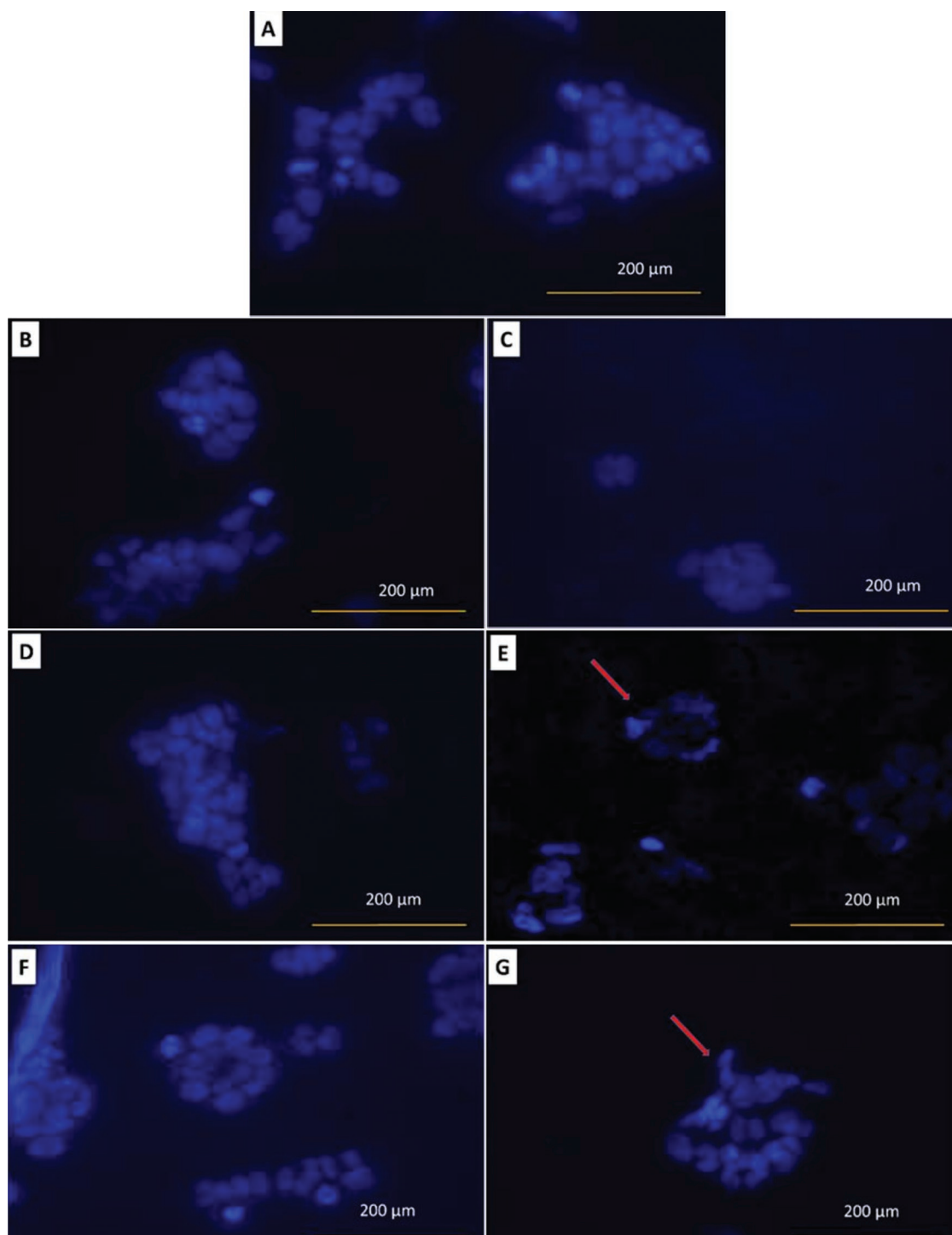


Figure 6. Microphotographs of HEK293 nuclear morphology stained with Hoechst at day 2 of culture. A) Polystyrene surface (control), B) PNIPAM, C) PNIPAM-co-20%HMA, D) PNIPAM-co-2%AMPS, E) PNIPAM-co-10%AMPS, F) PNIPAM-co-3%APTA, G) PNIPAM-co-10%APTA.

that both fractions (mitotic and fragmentation) are equivalent for both hydrogels, indicating a possible stagnation in cell growth. HEK293 nuclear alterations can be observed by means of microphotographs with Hoechst staining. The images in Figure 7C,D,E show the mitosis and fragmented nuclei, indicated by orange and green arrows, respectively.

These results suggest that the alteration in cell mitosis number and the presence of a higher number of fragmented nuclei observed in PNIPAM-co-10%AMPS and PNIPAM-co-10%APTA could be a consequence of low cell-hydrogel cohesion and rejecting of surface (Figure 5E,G). The observed behaviors are another piece of evidence that confirm the interfacial

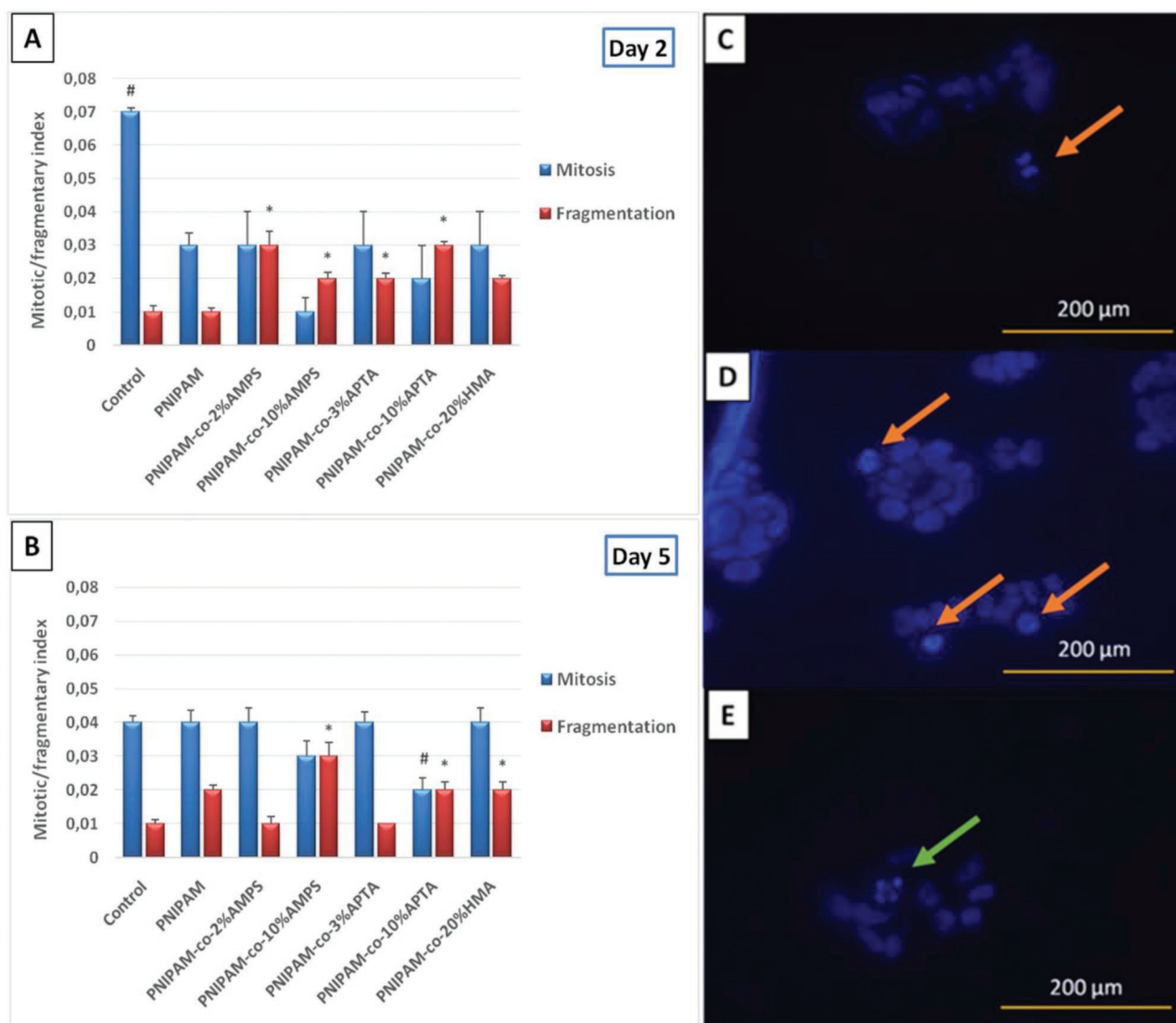


Figure 7. Fraction of mitotic and fragmented HEK293 nuclei with respect to the total population sample, at culture A) day 2 and B) 5. Each bar expresses the mean \pm S.E. of three independent experiments, each performed in duplicate. Data were analyzed by one way ANOVA and the differences were considered statistically significant with $p < 0.05$. *Statistically significant differences between fragmentation bars, and #statistically significant differences between mitotic bars. Hoechst-stained microphotographs of HEK293 nuclear alteration: C) PNIPAM; D) PNIPAM-co-3% APTA, and E) PNIPAM-co-2% AMPS. Orange arrows indicate nuclei in mitosis while green arrows design fragmented nuclei.

dependence between a specific cell or tissue growth and the physicochemical characteristics of surfaces.^[48,49]

2.5. Cell Cycle Progression after Adhesion on PNIPAM by Flow Cytometry

Cell cycle regulates mitotic division and therefore cell proliferation. This parameter could be affected by external factors like the mechanotransduction mechanism, when the cells sense and respond to external mechanical stimuli converting them in biochemical signals. The proportion of nuclei found in each of the phases (G0/G1, S, and G2) can be estimated to analyze the cycle progression. For that reason, the fluorescence analysis

of cell DNA stained with propidium iodide (PI) can be identified by flow cytometry. However, this assay can be applied to systems with high cell proliferation due to the cell number required by the cytometer. Thus, only HEK293 cells adhered to PNIPAM and polystyrene surfaces after 5 culture days were analyzed.

Results observed in **Figure 8** demonstrate that PI intensity in G0/G1, S, and G2 phases is similar in cells adhered on both surfaces, indicating that there are no alterations of the cell cycle after 5 days of proliferation. Therefore, the physicochemical properties of PNIPAM surfaces do not alter the proliferation of cells, allowing the normal cell division. This confirms the good biocompatibility of this material with the HEK293 culture.

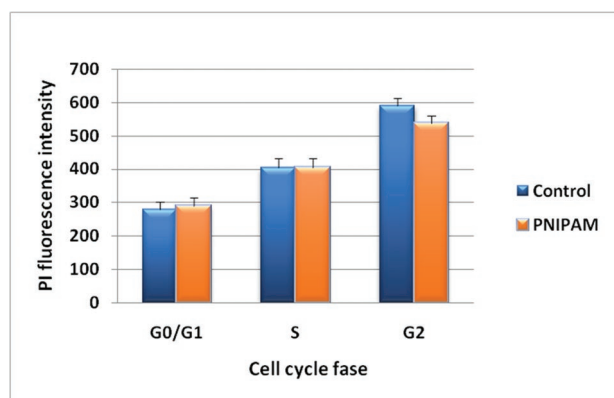


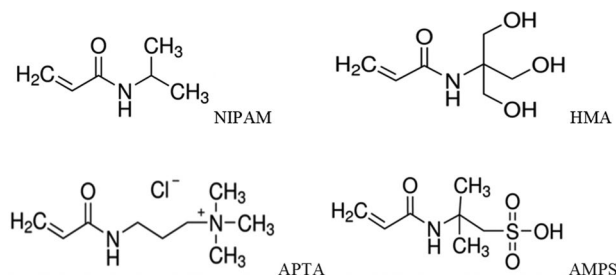
Figure 8. Proportion of HEK293 cells in each phase of cell cycle after 5 culture days. Each bar expresses the mean \pm S.E. of PI fluorescence intensity found in each phase of cell adhered on PNIPAM and polystyrene surfaces, from two independent experiments. Data were analyzed by one way ANOVA and the differences were considered statistically significant with $p < 0.05$.

3. Conclusions

Noncytotoxicity and presence of normal proliferation was proved for all hydrogels in periods of 96 and 48 h, respectively. Adhesion and proliferation of HEK293 on synthesized hydrogel surfaces were analyzed according to cell–matrix interactions and considering some of the physicochemical characteristics of the biointerfaces. Wettability, phase transition temperature, culture medium effect, and chemical composition of hydrogels were the parameters considered. However, other parameters as rigidity, rugosity, or porosity of surface could also be taken into account for the study of biological behavior of cell–material systems. It is known that a hydrogel with molecular porosity is obtained by the applied synthetic method.^[50] Therefore, the cells would observe a flat surface. Regarded to the rigidity of hydrogel could be controlled by crosslinker percentage, but in this study, it is not considered a variable parameter due to it was kept constant.

Cell adhesion changes throughout the days of culture due to surface adaptation. Hydrogel surfaces with neutral and low ionic charges allow a suitable cell adhesion, being the cells easily adapted and adhered with normal cell morphology (epithelial). The cell proliferation over PNIPAM also progresses without affecting the cell cycle. Whereas, ionic hydrogel surfaces with a higher net charge tend to inhibit the cell adhesion, showing rounded cytoplasmic morphology with cell–cell stronger interactions, anomaly nuclear morphology, and a major fragmentation index. It is noteworthy how the positive charges on the surface provoke a high effect over HEK293 growth.

Therefore, this type of cells adapts more easily over materials with hydrophobic superficial characteristics similar to control surfaces (polystyrene) and when the surface has enough cationic charge, they tend to reject it. Therefore, neutral and low ionic charges hydrogels have potential as scaffolds to future studies with renal origin cells. In addition, these results confirm that the adhesion and proliferation capacity of cell lines are defined by the cell–material scaffold biointerfacial characteristics.



Scheme 2. Chemical structures of used vinylic monomers.

4. Experimental Section

Materials: N-isopropylacrylamide (NIPAM), 2-acrylamido-2-methylpropanesulfonic acid (AMPS) were purchased from Scientific Polymer Products. (3-acrylamidopropyl)trimethylammonium chloride (APTA), N-acryloyl-tris-(hydroxymethyl)aminomethane (HMA), N,N-methylene bisacrylamide (BIS), ammonium persulfate (APS), and N,N,N',N'-tetramethylethylenediamine (TEMED) were purchased from Sigma-Aldrich. Chemical structures of vinylic monomers are shown in **Scheme 2**. DMEM (Invitrogen), FBS (Gibco), and antibiotic/antimycotic (penicillin, streptomycin, and amphotericin, Gibco) were used.

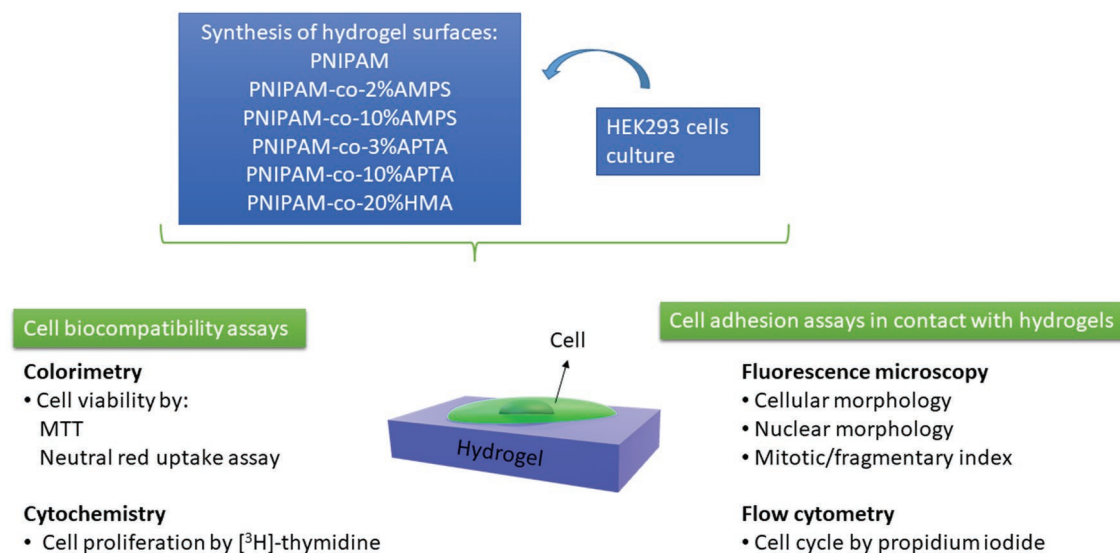
Experimental Design: The experimental design is summarized in **Scheme 3**. HEK293 cells were exposed to surfaces of PNIPAM and copolymers PNIPAM-co-2%AMPS, PNIPAM-co-10%AMPS, PNIPAM-co-3%APTA, PNIPAM-co-10%APTA, and PNIPAM-co-20%HMA for different periods of times, depending on each experiment. Complete DMEM medium supplemented with 10% FBS and 1% antibiotic/antimycotic was used. Cells were also seeded in polystyrene dishes as control surface. Study of cell cytotoxicity (MTT and Neutral Red Uptake) and cell proliferation (^3H -thymidine assay) was carried out at 48 and 96 h. On the other hand, HEK293 cells were seeded on the hydrogel surface and then biological parameters such as cellular and nuclear morphology, mitotic/fragmentation index, and cell cycle were analyzed.

Synthesis and Sterilization of Hydrogel Surfaces: PNIPAM surfaces were synthesized via free radical polymerization from 0.5 M of NIPAM solution with 2% moles (based on NIPAM moles) of BIS as crosslinker agent in distilled water. Next, the initiator system (1 mg mL⁻¹—APS and 10 μL mL⁻¹—TEMED) was added to the prepolymeric solution and O₂ was removed by bubbling with N₂ gas. Copolymers of NIPAM were synthesized by the addition of different percentage of comonomers to the prepolymeric solution, as indicated in **Table 2**, before adding the initiator system.

Prepolymeric solution was transferred into a 24-well top cover and the reaction was carried out at room temperature (22–25 °C) for 24 h, in order to obtain thin hydrogel surfaces. Once the synthesis process was finished, the surfaces were thawed and washed with distilled water for 5–7 days at room temperature, replacing the water several times to remove unreacted chemicals.

Prior to cell culture experiments, the swollen cylindrical hydrogel films (diameter: 1.5 cm, length: 0.2 cm) were dried in an oven at 50 °C during \approx 24 h until removing remaining water. Briefly, the surfaces were exposed to 70% ethanol during 10 min. Then the sterilization process was carried out in three steps. First, hydrogels were washed twice during 30 min in sterile phosphate saline solution (PBS, pH 7.3) to remove the ethanol. After, these were sterilized with PBS 10% v/v of antibiotic/antimycotic (10 000 UI mL⁻¹ penicillin, 10 000 μg mL⁻¹ streptomycin, 25 μg mL⁻¹ amphotericin B, Gibco). Finally, hydrogels were washed three times (30 min each) in sterile PBS to remove traces of the antibiotic/antimycotic. Then, films were immersed in culture medium (DMEM-10%FBS) during 24 h before seeding.

Physicochemical Characterization: FTIR: FTIR spectra were measured in a Nicolet Impact 400 spectrometer (Nicolet Instrument Corporation, Madison, WI, USA). The dry hydrogel samples were crushed and mixed with dry KBr salt to form pills under pressure and vacuum.



Scheme 3. Schematic representation of experimental design.

Static contact angle measurements: Water drop (0.1 mL) was placed over the hydrogel surface by sessile drop method and the internal contact angle was determined between the liquid–air interface line and the hydrogel surface.

In order to study the effect of culture medium on spatial rearrangement of functional groups of hydrogel surfaces, experiments were carried out for hydrogels swollen in water and supplemented DMEM medium. In addition, the experiments were also carried out on a heating plate at a controlled temperature of 37.0 ± 0.5 °C. So, the changes of superficial wettability in culture conditions were analyzed by measurement of contact angle with an Optical Tensiometer Theta Lite (Biolin Scientific).

Swelling capacity of hydrogels: Swelling percentages in equilibrium state ($\%Sw_{(eq)}$) were analyzed in order to define if the swelling affected the spatial disposition of the group functional of hydrogels. These were analyzed at 22 and 37 °C in a supplemented DMEM medium.

$\%Sw_{(eq)}$ was defined as the difference between mass of swollen (maximum capacity: m_{sw}) and dry hydrogel (m_{dry}) with respect to mass of dry hydrogel

$$\%Sw_{(eq)} = \frac{(m_{sw} - m_{dry})}{m_{dry}} \times 100 \quad (1)$$

Biologic Determinations: In vitro HEK293 cell culture: Human embryonic kidney cells (HEK293), an epithelial morphology cell line, was used in this work to analyze the biocompatibility and toxicity due to contact with hydrogels. Cells were cultured in DMEM supplemented with 10% FBS and 1% antibiotic/antimycotic at 37 °C in a humidified

Table 2. Percent composition of NIPAM and comonomer moles used for the polymeric synthesis.

Hydrogels	Moles percentages of monomers			
	NIPAM	AMPS	APTA	HMA
PNIPAM	100			
PNIPAM-co-2%AMPS	98	2		
PNIPAM-co-10%AMPS	90	10		
PNIPAM-co-3%APTA	97		3	
PNIPAM-co-10%APTA	90		10	
PNIPAM-co-20%HMA	80			20

atmosphere of 5% CO₂ in air. When they reach 70% to 80%, confluences were treated with trypsin (trypsin 0.5%, Sigma-Aldrich) to detach cells of substrate and used to perform the following experiments.

Cytotoxicity tests: Cell viability was assessed by MTT and Neutral Red uptake assays, on HEK293 cells exposed to hydrogels by contact at 48 and 96 h. MTT assay evaluated mitochondrial function through the reduction of MTT in a colored formazan salt by mitochondrial enzymes,^[51] while Neutral Red uptake assay was an indicator of viable cell's ability to incorporate and bind the dye into functional lysosomes.^[52]

Cells were seeded at 5×10^3 cells per well of 96-well plate. After 24 h, cylindrical films (diameter: 0.5 cm, length: 0.2 cm) were deposited over the culture medium and incubated for 48 and 96 h at 37 °C. Negative (polystyrene surface) and positive (DMSO:DMEM 10%FBS, 1:9, adapted from Da Violante et al.)^[53] controls were included. Then, hydrogels were removed and MTT solution (0.5 mg mL⁻¹ in complete medium) or Neutral Red dye (1 mg mL⁻¹ in complete medium) was added and incubated for 3 h at the same temperature in the dark. The medium of each well was removed and replaced by 100 µL of DMSO or 100 µL of a C₂H₅OH:CH₃COOH solution (50:1). The absorbance of both dyes was recorded by a microplate reader (Bio-Rad, Hercules, CA, USA) at 540 nm. The viable cell number was expressed as OD (optical density) of Formazan or Neutral Red dyes obtained from exposed cells and control groups.

[³H]-thymidine assay: HEK293 proliferation was determined by the [³H]-thymidine assay of exposed cells and on negative (only DMEM-10%FBS) control. This assay was able to detect the incorporation of the tritium-labeled thymidine nucleotide into DNA strands synthesized de novo.^[54] After 24 h of seeding (5×10^3 cells per well in a 96-well plate), cells were covered with hydrogels (diameter: 0.5 cm, length: 0.2 cm) and cultivated in the presence of [³H]-thymidine/DMEM (PerkinElmer, Boston, MA, USA) during 24 and 48 h. Moreover, cells were harvested, DNA samples were obtained in a glass filter paper and later diluted in a liquid scintillation cocktail (PerkinElmer, Loughborough Leics, England). A liquid Scintillation β Counter (Beckman LS 60001 C; Fullerton, CA, USA) was used to measure the [³H]-thymidine. Cell proliferation at 24 and 48 h was expressed as counts per minute (cpm) of [³H]-thymidine for cells exposed to hydrogel and control groups.

Seeding method on hydrogels films: The biomaterial's chemical structure and the behavior of adhered cells are two of the most important parameters to take into account in cell–material interaction and adhesive/attachment characteristics evaluation. Cell and nucleus morphology, distribution, mitotic/fragmentation index, and cell cycle were analyzed after 5 days of cell adhesion on surfaces.

First, hydrogel films (diameter: 1.5 cm, length: 0.2 cm) were dried to eliminate the rest of sterilization solutions and swelled in DMEM-10% FBS during 24 h prior cell seeding. Second, HEK293 cells were seeded at a density of 2.5×10^4 cells per hydrogel, inside a 24-well microplate, and cultivated for a period of 5 days. Cells growth on polystyrene traditional surfaces was included as control, following the same process as hydrogel treatment.

Cytoplasmic and nuclear distribution and morphologies: In order to observe if cell–material interaction changed the cytoplasmic or nuclear phenotype of HEK293 attached to the hydrogel surface after 2 and 5 days of culture, Acridine Orange and Hoechst 33258 staining techniques were used, respectively. Samples were fixed with cold 4% formaldehyde/PBS (4 °C) for 10 min and then $1 \mu\text{g mL}^{-1}$ Acridine Orange solution was added to cover the pieces for 15 min. For nuclei visualization, fixation with cold methanol at -20°C during 10 min was made for later staining with a $20 \mu\text{L mL}^{-1}$ solution of Hoechst 33258/PBS (1 mg mL^{-1}). Films were washed with PBS and observed by inverted fluorescence microscopy under UV light, using an optical inverted fluorescence microscopy (Nikon Eclipse model Ti-S 100 (Nikon, Japan)) with a coupled digital capture camera (Nikon, Japan). Fluorescence intensity of Acridine Orange was measured with excitation and emission wavelengths of 520 and 650 nm, respectively. For the assay with Hoechst 33258, the excitation and emission wavelengths of 345 and 446 nm were used.

Based on the acquired fluorescent images, nuclei with mitotic and fragmentary characteristics were identified. At total of 200 nuclei per sample were counted in different fields and mitotic/fragmentary index was calculated.^[55]

Cell cycle by flow cytometry: Cell cycle distribution analysis of HEK293 adhered to PNIPAM surface was carried out through PI staining (Sigma) and read by flow cytometry. At 5 culture day, cells were harvested by trypsinization, collected by centrifugation, fixed overnight with 100% ethanol at -20°C , and incubated with $5 \mu\text{g mL}^{-1}$ PI/PBS and 0.015 U mL^{-1} RNase in PBS during 20 min at room temperature in the dark. Fluorescence intensity of PI was analyzed in a Guava flow cytometer (guava easyCyte System, Merck KGaA, Darmstadt, Germany) with excitation and emission wavelengths setting at 484 and 500 nm, respectively. Results were modeled using the Cyflog software (PerttuTerho, Mika Korkeamaki, CyFlo Ltd.) and expressed as fluorescence intensity of PI of HEK293 cells.

Statistical Analysis: To eliminate outliers, the data obtained in all quantitative tests were analyzed using the box plot test. The values were expressed as means \pm S.E. with a minimum of three independent repetitions per experiment. Data were evaluated by one-way analysis of variance (ANOVA) and Bonferroni post hoc test. Differences were considered significant at $p < 0.05$ using the INFSTAT/L program.^[56]

Supporting Information

Supporting Information is available from the Wiley Online Library or from the author.

Acknowledgements

Research was funded by grants from National University of Río Cuarto (UNRC) through the Science and Technology Secretary (SECYT), Fund for Scientific and Technological Research (FONCYT), and National Council of Scientific and Technical Research (CONICET).

Conflict of Interest

The authors declare no conflict of interest.

Data Availability Statement

The data that support the findings of this study are available from the corresponding author upon reasonable request.

Keywords

biocompatibility, cell adhesion, hydrogel surfaces, interfaces, ionic surfaces

Received: May 25, 2022

Revised: August 29, 2022

Published online:

- [1] E. M. Ahmed, *J. Adv. Res.* **2015**, 6, 115.
- [2] H. Yuk, B. Lu, X. Zhao, *Chem. Soc. Rev.* **2019**, 48, 1642.
- [3] H. Geckil, F. Xu, X. Zhang, S.-J. Moon, U. Demirci, *Nanomedicine* **2010**, 5, 469.
- [4] E. C. González-Díaz, S. Varghese, *Gels* **2016**, 2, 20.
- [5] D. Rana, T. S. Sampath Kumar, M. Ramalingam, *J. Biomater. Tissue Eng.* **2014**, 4, 507.
- [6] S. Tang, H. Ma, H.-C. Tu, H.-R. Wang, P.-C. Lin, K. S. Anseth, *Adv. Sci.* **2018**, 5, 273.
- [7] B. N. Narasimhan, M. S. Horrocks, J. Malmström, *Adv. NanoBiomed Res.* **2021**, 1, 2100059.
- [8] W. Zhang, R. Wang, Z.-M. Sun, X. Zhu, Q. Zhao, T. Zhang, A. Cholewinski, F. K. Yang, B. Zhao, R. Pinnaratip, P. K. Forooshani, B. P. Lee, *Chem. Soc. Rev.* **2020**, 49, 433.
- [9] J. Tavakoli, Y. Tang, *Polymers* **2017**, 9, 364.
- [10] E. Karjalainen, V. Aseyev, H. Tenhu, *Polym. Chem.* **2015**, 6, 3074.
- [11] X. Li, Q. Sun, Q. Li, N. Kawazoe, G. Chen, *Front. Chem.* **2018**, 6, 499.
- [12] R. E. Rivero, F. Alustiza, N. Rodríguez, P. Bosch, M. C. Miras, C. R. Rivarola, C. A. Barbero, *React. Funct. Polym.* **2015**, 97, 77.
- [13] R. Rivero, F. Alustiza, V. Capella, C. Liaudat, N. Rodríguez, P. Bosch, C. Barbero, C. Rivarola, *Colloids Surf., B* **2017**, 158, 488.
- [14] A. Vedadghavami, F. Minooei, M. Hossein, S. Khetani, A. Rezaei, S. Mashayekhan, A. Sanati-Nezhad, *Acta Biomater.* **2017**, 62, 42.
- [15] M. A. Haq, Y. Su, D. Wang, *Mater. Sci. Eng., C* **2017**, 70, 842.
- [16] H. Vihola, A. Laukkanen, L. Valtola, H. Tenhu, J. Hirvonen, *Biomaterials* **2005**, 26, 3055.
- [17] L. Yang, F. Cheng, T. Liu, J. R. Lu, K. Song, L. Jiang, S. Wu, W. Guo, *Biomed. Mater.* **2012**, 7, 035003.
- [18] R. E. Rivero, V. Capella, A. C. Liaudat, P. Bosch, C. A. Barbero, N. Rodríguez, C. R. Rivarola, *RSC Adv.* **2020**, 10, 5827.
- [19] V. Capella, R. E. Rivero, A. C. Liaudat, L. E. Ibarra, D. A. Roma, F. Alustiza, F. Mañas, C. A. Barbero, P. Bosch, C. R. Rivarola, N. Rodríguez, *Heliyon* **2019**, 5, e01474.
- [20] W. Li, Z. Yan, J. Ren, X. Qu, *Chem. Soc. Rev.* **2018**, 47, 8639.
- [21] D. Seliktar, *Science* **2012**, 336, 1124.
- [22] S. Terry, F. Jouret, F. Vandenabeele, I. Smolders, M. Moreels, O. Devuyst, P. Steels, E. Van Kerkhove, *Am. J. Physiol.: Renal Physiol.* **2007**, 293, F476.
- [23] H. Zhang, S. F.-T. Lau, B. F. Heng, P. Y. Teo, P. K. D. Thilini Alahakoon, M. Ni, F. Tasnim, J. Y. Ying, D. Zink, *J. Cell. Mol. Med.* **2011**, 15, 1287.
- [24] Y.-C. Lin, M. Boone, L. Meuris, I. Lemmens, N. Van Roy, A. Soete, J. Reumers, M. Moisse, S. Plaisance, R. Drmanac, J. Chen, F. Speleman, D. Lambrechts, Y. Van de Peer, J. Tavernier, N. Callewaert, *Nat. Commun.* **2014**, 31, 71.
- [25] R. M. Silverstein, F. X. Webster, *Spectrometric Identification of Organic Compounds*, John Wiley and Sons Inc, New York **1988**.
- [26] R. Casadey, M. Broglia, C. Barbero, S. Criado, C. Rivarola, *React. Funct. Polym.* **2020**, 156, 104729.

- [27] M. F. Broglia, I. Balmaceda, F. Carrizo, C. A. Barbero, C. R. Rivarola, *Mater. Res. Express* **2019**, 6, 055021.
- [28] Y. C. Jung, B. Bhushan, *Nanotechnology* **2006**, 17, 4970.
- [29] J. Litowczenko, J. Gapiński, R. Markiewicz, A. Woźniak, J. K. Wychowaniec, B. Peplińska, S. Jurga, A. Patkowski, *Mater. Sci. Eng., C* **2021**, 118, 111507.
- [30] I. Sanzari, E. Buratti, R. Huang, C. G. Tusan, F. Dinelli, N. D. Evans, T. Prodromakis, M. Bertoldo, *Sci. Rep.* **2020**, 10, 6126.
- [31] J. Cusick, A. Mustian, K. Goldberg, M. E. Reyland, *Cell. Immunol.* **2010**, 261, 1.
- [32] G. S. Hussey, J. L. Dziki, S. F. Badylak, *Nat. Rev.* **2018**, 3, 159.
- [33] M. V. Martinez, S. Bongiovanni Abel, R. Rivero, M. C. Miras, C. R. Rivarola, C. A. Barbero, *Polymer* **2015**, 78, 94.
- [34] B. V. Slaughter, S. S. Khurshid, O. Z. Fisher, A. Khademhosseini, N. A. Peppas, *Adv. Mater.* **2009**, 21, 3307.
- [35] J. Fukuda, A. Khademhosseini, Y. Yeo, X. Yang, J. Yeh, G. Eng, J. Blumling, C.-F. Wang, D. S. Kohane, R. Langer, *Biomaterials* **2006**, 27, 5259.
- [36] G. B. Schneider, A. English, M. Abraham, R. Zaharias, C. Stanford, J. Keller, *Biomaterials* **2004**, 25, 3023.
- [37] R. Iwai, R. Haruki, Y. Nemot, Y. Nakayama, *J. Biomed. Mater. Res., Part B* **2017**, 105B, 1009.
- [38] F. Tan, J. Liu, M. Liu, J. Wang, *Mater. Sci. Eng., C* **2017**, 76, 330.
- [39] A. Schulz, A. Katsen-Globa, E. J. Huber, S. C. Mueller, A. Kreiner, N. Pütz, M. M. Gepp, B. Fischer, F. Stracke, H. von Briesen, J. C. Neubauer, H. Zimmermann, *J. Mater. Sci.: Mater. Med.* **2018**, 29, 105.
- [40] P. M. Chou, P. S. Khiew, P. D. Brown, B. Hu, *Polymers* **2021**, 13, 2629.
- [41] J. Ishikawa, H. Tsuji, H. Sato, Y. Gotoh, *Surf. Coat. Technol.* **2007**, 201, 8083.
- [42] J. D. Mendelsohn, S. Y. Yang, J. Hiller, A. I. Hochbaum, M. F. Rubner, *Biomacromolecules* **2003**, 4, 96.
- [43] S.-H. Hsu, G.-S. Huang, *Biomaterials* **2013**, 34, 4725.
- [44] B. Sarker, R. Singh, R. Silva, J. A. Roether, J. Kaschta, R. Detsch, D. W. Schubert, I. Cicha, A. R. Boccaccini, *PLoS One* **2014**, 9, e107952.
- [45] A. L. Hillberg, C. A. Holmes, M. Tabrizian, *Biomaterials* **2009**, 30, 4463.
- [46] L. Gao, H. Gan, Z. Meng, R. Gu, Z. Wu, L. Zhang, G. Dou, *Colloids Surf., B* **2014**, 117, 398.
- [47] D. M. Graham, K. Burridge, *Curr. Opin. Cell Biol.* **2016**, 40, 98.
- [48] K. L. Christman, *Science* **2019**, 363, 340.
- [49] L. Ghasemi-Mobarakeh, D. Kolahreez, S. Ramakrishna, D. Williams, *Curr. Opin. Biomed. Eng.* **2019**, 10, 45.
- [50] M. A. Molina, C. R. Rivarola, M. C. Miras, D. Lescano, C. A. Barbero, *Nanotechnology* **2011**, 22, 245504.
- [51] T. Mossman, *J. Immunol. Methods* **1983**, 65, 55.
- [52] E. Borenfreund, J. A. Puerner, *Toxicol. Lett.* **1985**, 24, 119.
- [53] G. Da Violante, N. Zerrouk, I. Richard, G. Provot, J. C. Chaumeil, P. Arnaud, *Biol. Pharm. Bull.* **2002**, 25, 1600.
- [54] P. K. Bond, V. P. Flidner, T. M. Cronkite, E. P. Rubini, J. R. Brecher, G. Schork, *Acta Haematol.* **1959**, 21, 1.
- [55] C. Nakanishi, N. Nagaya, S. Onhishi, K. Yamahara, S. Takabatake, T. Konno, K. Hayashi, M. Kawashiri, T. Tsubokawa, M. Yamagishi, *Circ. J.* **2011**, 75, 2260.
- [56] J. A. Di Rienzo, F. Casanoves, M. G. Balzarini, L. Gonzalez, M. Tablada, C. W. Robledo, *InfoStat Versión 2018. Grupo InfoStat, FCA, Universidad Nacional de Córdoba, Argentina* **2020**.